Analyst

PAPER

View Article Online
View Journal | View Issue

Cite this: *Analyst*, 2015, **140**, 4576

A near-infrared fluorescent probe for the selective detection of HNO in living cells and *in vivo*†

Ping Liu,‡[a] Xiaotong Jing,‡[a] Fabiao Yu,*[a,b] Changjun Lv[b] and Lingxin Chen*[a,b]

Received 18th April 2015,
Accepted 1st May 2015

DOI: 10.1039/c5an00759c

www.rsc.org/analyst

Nitroxyl (HNO), the one-electron reduced and protonated analogue of nitric oxide (NO), demonstrates distinctive bio-pharmacological effects in the treatment of cardiovascular disorders. Herein, we design and synthesize a near-infrared (NIR) metal-free fluorescent probe Cyto-JN for the detection of nitroxyl (HNO) in living cells and *in vivo*. The metal-free Cyto-JN is composed of two moieties: the Aza-BODIPY fluorophore and the HNO recognition unit, the diphenylphosphinobenzoyl group. Cyto-JN can react with HNO in a 1 : 1 stoichiometry, which may bring great benefit to the detection efficiency of bioassays. Cyto-JN shows high sensitivity toward HNO and exhibits low cytotoxic effect on cells. Moreover, the probe displays good selectivity for the detection of HNO in the presence of various biologically related species. Cyto-JN can be applied successfully to bio-imaging of HNO in living cells and in mice. The results of flow cytometry confirm that the probe Cyto-JN can be used to detect intracellular HNO qualitatively and quantitatively.

Introduction

Nitroxyl (HNO), the one-electron reduced and protonated analogue of nitric oxide (NO), has drawn lots of attention due to its potential bio-pharmacological effects.[1] HNO may possess some unique and favorable properties, which are relevant in the treatment of cardiovascular disorders such as angina, acute hypertensive crises and atherosclerosis.[1] Some reports confirm that Angeli's salt (an HNO donor) is a potent vasodilator both *in vitro* and *in vivo*, which can elicit vasorelaxation in an isolated large conduits,[2–5] small resistance arteries[6] and intact coronary vessels.[7] In addition, HNO demonstrates distinct actions on myocardial contractile function that differ from NO. It can target cardiac sarcoplasmic ryanodine receptors to increase myocardial contractility.[8–10] This pharmacological effect may provide a promising therapy for heart failure and effectively avoid the problem of nitrate tolerance. Despite the accumulating evidences of the bio-pharmacological importance of HNO, deep explorations of endogenous HNO functional mechanisms in cells are hampered by the lack of efficacious detection methods, because HNO can rapidly dimerize and dehydrate to nitrous oxide (N_2O) in biological systems.[1,2,11]

Early methods of detecting HNO mainly include electrochemistry, electron paramagnetic resonance (EPR), colorimetry, and chemiluminescence.[12] Compared with these detection techniques, the fluorescent probe has been recognized as a preferred detection technology for the detection of bio-reactive species *in situ* in biological systems due to its non-invasiveness and high spatiotemporal resolution.[13] Hitherto, a few fluorescent probes for HNO detection have been reported, but they are mainly based on a Cu^{2+}-mediated process.[14–17] Although efforts have been made in the development of HNO fluorescent probes, these metal-mediated HNO probes trend to be interfered by biological reductants such as glutathione (GSH) and ascorbate, which are abundant in living cells. In addition, the excitation/emission wavelengths of these developed probes mainly locate in the UV-visible region, which will suffer obstruction from background autofluorescence. However, near-infrared (NIR) light (650–900 nm) can penetrate tissues more deeply to minimize photo damage and avoid noise from background autofluorescence.[18] Therefore, a probe that not only detects HNO with high selectivity but also emits in the NIR region of the spectrum is more desirable. Herein, we designed and synthesized a NIR fluorescent probe, Cyto-JN, for HNO detection in living cells and *in vivo* (Scheme 2). The metal-free Cyto-JN would detect HNO with a 1 : 1 stoichiometry, which will benefit the detection efficiency of the probe in bioassays. Cyto-JN responded to HNO sensitively and selectively with low cytotoxicity. Moreover, Cyto-JN was applied successfully to visualize HNO in living cells and in mice. The

[a]*Key Laboratory of Coastal Environmental Processes and Ecological Remediation; The Research Center for Coastal Environmental Engineering and Technology, Yantai Institute of Coastal Zone Research, Chinese Academy of Sciences, Yantai 264003, China. E-mail: fbyu@yic.ac.cn, lxchen@yic.ac.cn*

[b]*Medicine Research Center, Binzhou Medical University, Yantai 264003, P.R. China*

†Electronic supplementary information (ESI) available: Experimental supplementary methods for chemical synthesis and characterization of compounds. See DOI: 10.1039/c5an00759c

‡These authors contributed equally.

results of flow cytometry confirm that our probe could be used to detect intracellular HNO qualitatively and quantitatively.

Results and discussion

Design and synthesis of Cyto-JN

The metal-mediated fluorescent probes for HNO detection are prone to be interfered by biological reductive species.[14–17] Fortunately, the reaction of HNO with triarylphosphines can produce the corresponding phosphine oxide and aza-ylides, which will undergo a Staudinger ligation to yield amides by the nitrogen atom nucleophilic attacking of *ortho*-ester.[19,20] The reaction may serve as a newly defined method for the detection of HNO in cells.[21–23] However, fluorescent probes, which employ the reaction of HNO with triarylphosphines, often suffer waste of half the dosage owing to the production of phosphine oxide (Scheme 1). We recognize that the high yields of the reaction of the probe with HNO should be particularly advantageous for the exact determination of endogenous HNO level changes in living cells. Based on the abovementioned considerations, we strived to develop a metal-free NIR fluorescent probe for intracellular HNO detection with a 1 : 1 stoichiometry (Scheme 1). As shown in Scheme 2, the probe Cyto-JN is composed of two moieties: the Aza-BODIPY fluorophore and the HNO recognition unit, the diphenylphosphinobenzoyl group. Aza-BODIPY was chosen as fluorophore because the NIR dye exhibited good membrane permeability, high fluorescence quantum yield and good resistance to photo bleaching. When reacted with HNO, one diphenylphosphinobenzoyl group produced phosphine oxide and the other one formed aza-ylide, and the aza-ylide would nucleophilically attack the carbonyl of the ester, resulting in the release of Cyto-JNO. As a result, the reaction of Cyto-JN with HNO was at 1 : 1 stoichiometry, which distinguished our probe from other metal-free probes at 2 : 1 stoichiometry.[21–23] The fluorophore Aza-BODIPY was prepared starting from 4′-hydroxychalcone.[22,24]

The synthesis of Cyto-JN was outlined in Scheme 3. The fluorophore Aza-BODIPY was synthesized based on a previously reported method[13i] (Scheme S1, ESI†). After the fluorophore Aza-BODIPY reacted with 2-(diphenylphosphino)

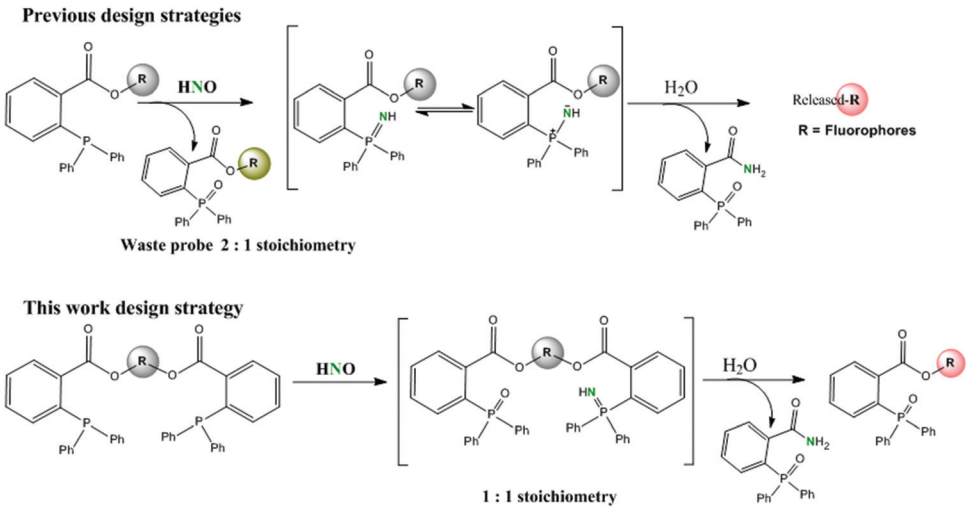

Scheme 1 The design strategies for the metal-free fluorescent probes.

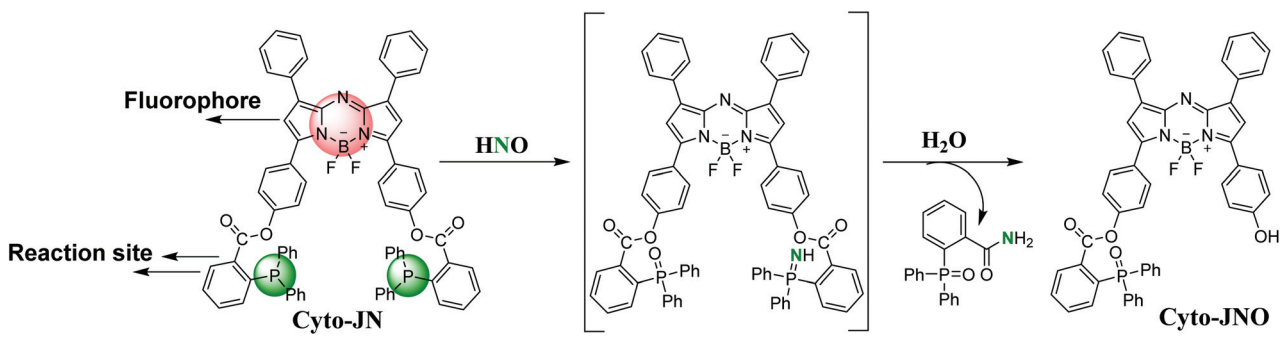

Scheme 2 Proposed reaction mechanism of Cyto-JN with HNO.

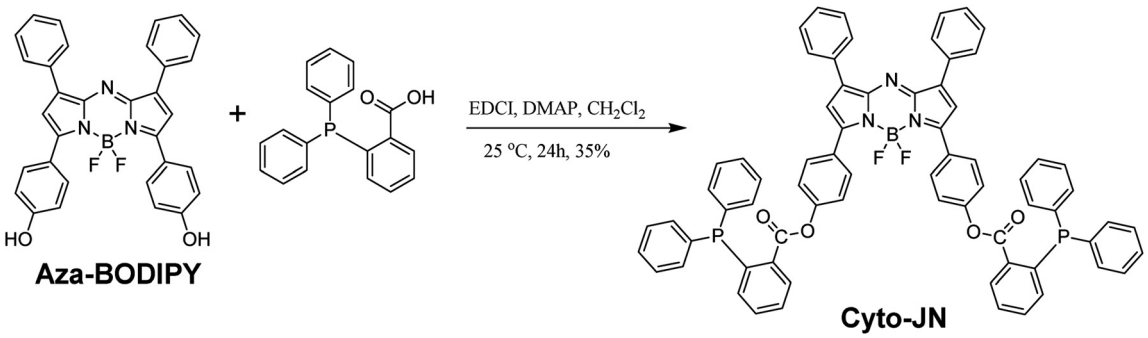

Scheme 3 Synthesis of Cyto-JN.

benzoic acid, the final probe Cyto-JN was yielded. The structures of compounds were characterized by ^{1}H NMR, ^{13}C NMR and MS (ESI).

Spectroscopic response of Cyto-JN to HNO

The absorption and fluorescence spectra of Cyto-JN (5 μM) were examined under simulated physiological conditions (10 mM HEPES buffer, pH 7.4), including 0.5% Tween 80 (Tw 80), because the environment of the cell is liposoluble, and Tw 80 is a nonionic surfactant and has been widely used in foods, pharmaceutical preparations, and cosmetics due to its effectiveness at low concentrations and relatively low toxicity. We employed 0.5% Tw 80 to simulate the hydrophobicity of the cells. The maximum absorption wavelength of Cyto-JN was at 672 nm (ε = 4.83 × 10^{4} M^{-1} cm^{-1}). Upon the addition of Angeli's salt (AS, a common HNO donor), the absorption at 672 nm decreased gradually, accompanied by an increase of the absorption peak centred at 706 nm (ε = 5.88 × 10^{4} M^{-1} cm^{-1}). The absorption spectra under different concentrations of AS displayed an isosbestic point at 682 nm (Fig. 1a). In some experimental protocols, it is desirable to choose the excitation wavelengths at the isosbestic point because isosbestic points can be used as a quality assurance method, which will provide a measure of events independent of interference factors such as light scatter, dye leakage or spectral profile changes.[25–27] Therefore, we selected the isosbestic point at 682 nm as the excitation wavelength. Fluorescence titration of Cyto-JN in the presence of AS with a concentration range from 0 to 10 μM was then performed. As shown in Fig. 1b, the corresponding fluorescence emission profiles increased with a centre at 734 nm. Both the excitation and the emission wavelengths of Cyto-JN were situated in the NIR region, indicating that our probe could greatly reduce background interference and improve the detection sensitivity. There was a linear concentration-dependent fluorescent response with Cyto-JN to AS ranging from 0 to 10 μM (Fig. 1b, inset), and the calibration curve was $F_{734\ nm}$ = 95.28 [AS] μM + 87.25 (r = 0.988). The detection limit for HNO was calculated to be 30 nM ($3\sigma/k$), indicating that our probe was highly sensitive to HNO. The quantum yields of Cyto-JN increased from 0.02 to 0.35. Because the environment *in vivo* is more complex, we next investigated the

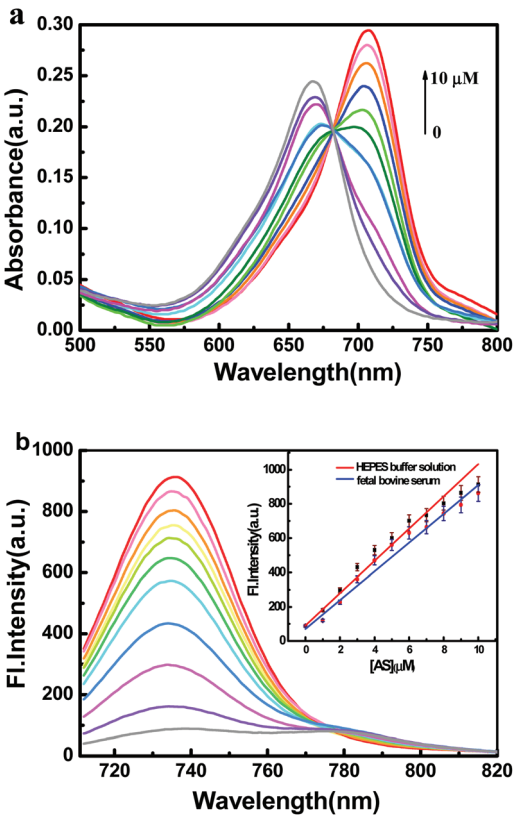

Fig. 1 (a) Absorption and (b) fluorescence spectra of Cyto-JN (5 μM) for various concentrations of AS (0, 1, 2, 3, 4, 5, 6, 7, 8, 9, 10 μM). The isosbestic point was at 682 nm. Fluorescence emission ranged from 710 to 820 nm. Inset: relationship between fluorescence intensity at 734 nm and AS concentrations. Spectra were acquired in HEPES buffer solution (10 mM, 0.5% TW 80, pH 7.4) and in serum (20%) after the incubation of Cyto-JN with AS for 20 min.

capability of Cyto-JN to detect HNO in serum samples. The examination was performed in a simulated solution containing 20% fetal bovine serum. Different concentrations of HNO (0–10 μM) were added to the samples containing 5 μM Cyto-JN. As shown in Fig. 1b, the fluorescence intensities at 734 nm were linearly related to the concentration of HNO under the given testing conditions. The regression equation was $F_{734\ nm}$ = 71.32

[AS] μM + 83.78 (r = 0.981). These results indicate that Cyto-JN has potential for HNO detection in cells and *in vivo*.

Selectivity of Cyto-JN to HNO

We next assessed the selectivity of Cyto-JN toward AS upon the addition of various typical biologically relevant species. The fluorescence responses to biologically relevant species were obtained at the time points 0, 5, 10, 15, and 20 min. As shown in Fig. 2, nearly no fluorescence intensity changes were observed in the presence of reactive oxygen species (ROS) and reactive nitrogen species (RNS), including $ONOO^-$, NO, NO_2^-, H_2O_2, O_2^-, ClO^-, and methyl linoleate hydroperoxide (MeLOOH). In addition, the fluorescence intensity of Cyto-JN was also hardly affected by biological reductants such as L-cysteine (Cys), glutathione (GSH), NaHS (source of H_2S), ascorbic acid (V_C), tocopherols (V_E), citrate, tyrosine (Tyr), or hydroxylamine (HA). Some researchers suggest that phosphines can also react with GSNO to yield aza-ylides in a fashion similar to HNO.[28] Therefore, GSNO may interfere with phosphine-based HNO detection. However, as shown in Fig. 2a, the fluorescence change caused by GSNO was comparatively slight, suggesting our probe showed good selectivity to HNO over GSNO. All these results demonstrate that Cyto-JN is highly selective for HNO over ROS, RNS, and biological reducing species. Therefore, the probe can meet the urgent requirements for the detection of HNO in complex biological samples.

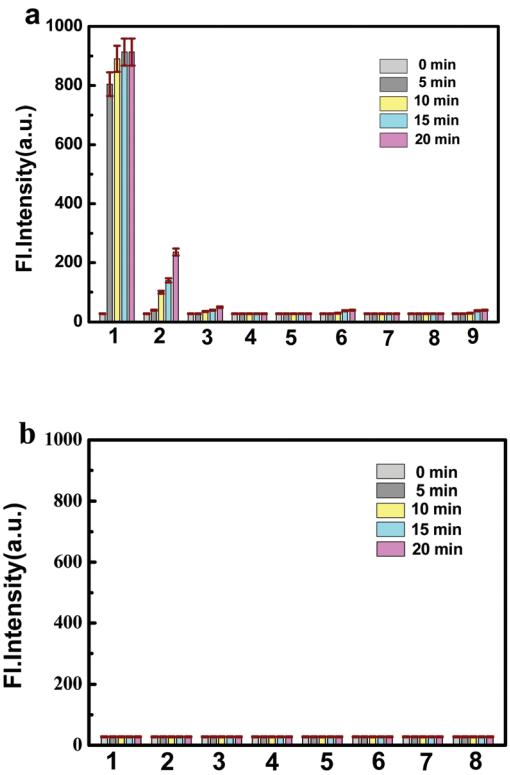

Fig. 2 Fluorescence responses of 5 μM Cyto-JN to test species in HEPES buffer solution (10 mM, pH 7.4, 0.5% TW 80). (a) 1, 10 μM AS; 2, 50 μM GSNO; 3, 500 μM $ONOO^-$; 4, 20 μM NO; 5, 500 μM NO_2^-; 6, 250 μM H_2O_2; 7, 100 μM O_2^-; 8, 20 μM MeLOOH; 9, 250 μM ClO^-. (b) 1, 50 μM Cys; 2, 100 μM GSH; 3, 500 μM NaHS; 4, 50 μM V_C; 5, 50 μM V_E; 6, 100 μM citrate; 7, 250 μM tyrosine (Tyr); 8, 50 μM HA. (λ_{ex} = 682 nm, λ_{em} = 734 nm).

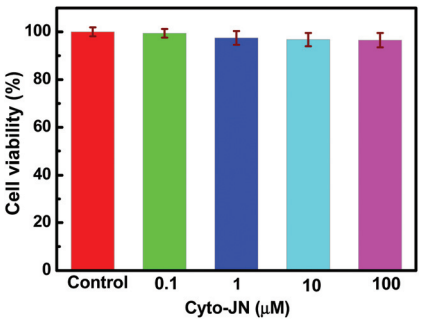

Fig. 3 Cell viabilities of Cyto-JN using RAW 264.7 cells as test model. Cells were treated with 0.1–100 μM of Cyto-JN for 24 h. Data were expressed as the means ± SD of data obtained from triplicate experiments.

Cytotoxic effect of Cyto-JN

Because low cytotoxicity is one of the key criteria for the physiological application of a fluorescent probe *in vivo*. We next evaluated the cytotoxicity of Cyto-JN by MTT assay using RAW 264.7 cells. As illustrated in Fig. 3, cell viabilities were over 90% even with the addition of 100 μM Cyto-JN for 24 h. The results demonstrate that our probe can provide low cytotoxicity for the biochemical tests in cells and *in vivo*.

Bioimaging of HNO in cells

On the basis of the high sensitivity and selectivity features of Cyto-JN for the detection of HNO in solution, we next explored its applicability for imaging HNO in living cells utilizing laser scanning confocal microscopy. We chose the cells in the same visual field as the test targets. After being incubated with 5 μM Cyto-JN at 37 °C for 15 min, the RAW 264.7 cells displayed faint fluorescence on imaging (Fig. 4a). The cells were washed with DMEM three times with a rinsing device to remove the overdose probe. Next, a dosage of 100 μM AS was added in the test system. After the treatment of the cells under 37 °C for 15 min, a strong intracellular fluorescence response was initiated (Fig. 4d). Given that Cyto-JN could respond to HNO with 1 : 1 stoichiometry, we then added another dosage of 100 μM AS into the cellular system to evaluate the detection capacity of Cyto-JN. As revealed in Fig. 4g, there existed one more fluorescence burst. The results suggest that our probe Cyto-JN has a high capacity for HNO detection when compared with the reported metal-free probes at the same dosage. We selected the cells in the visual field as the region of interest (ROI in Fig. 4a, d, and g). The average fluorescence intensities of the cells were determined with Image-Pro Plus software. Fig. 4j illustrated that the fluorescence intensity of quantification data in Fig. 4a, d, and g could clearly offer high dosage capacity toward HNO. We also adapted a colocation experi-

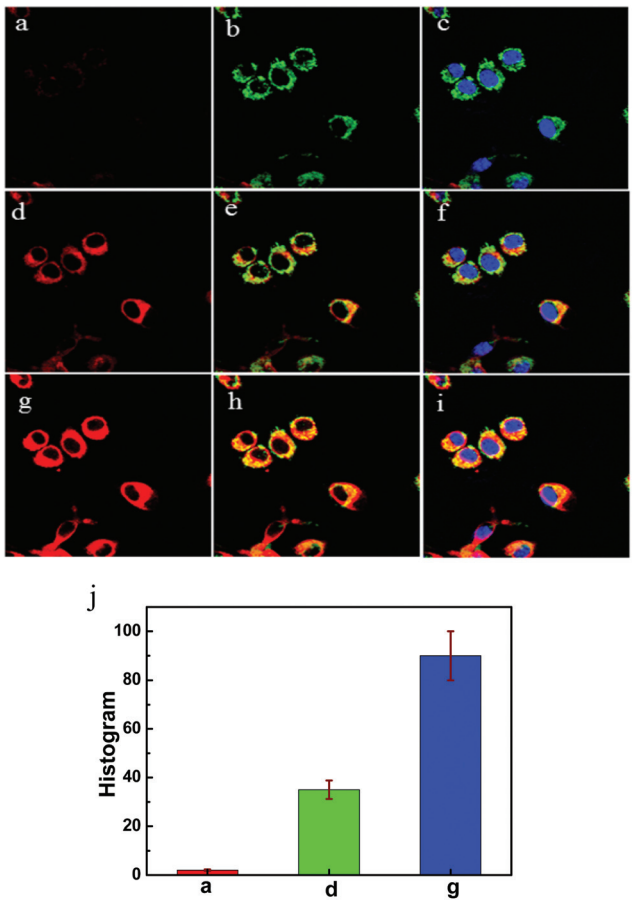

Fig. 4 Confocal fluorescence images of HNO in RAW 264.7 cells with Cyto-JN. (a) Cells loaded with 5 μM probe for 15 min. (d) Cells treated with 100 μM AS for 30 min. (g) Cells exposed to another 100 μM AS for an additional 30 min. Fluorescence collection window: λ_{ex} = 633 nm, λ_{em} = 700–800 nm; (b, e, and h) overlay of Cyto-JN channel and Calcein-AM channel. Fluorescence collection window: λ_{ex} = 488 nm, λ_{em} = 500–550 nm; (c, f, and i) overlay of Cyto-JN channel, Calcein-AM channel and Hoechst 33342 channel. Fluorescence collection window: λ_{ex} = 405 nm, λ_{em} = 420–480 nm; the abovementioned results are representative of five independent experiments; (j) quantification of the fluorescence intensity of ROI in a, d, and g. n = 5, error bars were ± SD.

ment to examine the intracellular location of Cyto-JN. We introduced a cytoplasm targetable dye, Calcein-AM, and a fluorescence marker, Hoechst 33342, for nuclei to discern the cellular location of Cyto-JN in RAW 264.7 cells. As shown in Fig. 4c, f and i, the fluorescence image of Cyto-JN exhibited a consistent overlap with Calcein-AM in cytoplasm, whereas the probe showed hardly any overlap with the nucleus dye Hoechst 33342. The results verify that Cyto-JN can potentially situate itself in the cytoplasm to detect HNO dynamic changes in cells and *in vivo*.

Flow cytometry analysis

A laser scanning confocal microscope analyzes a relatively small number of cells only in a visual field. Therefore, it may obtain false results for the detection systems. In order to further confirm the fluorescence changes in living cells caused by HNO, we carried out a flow cytometry assay to test and verify the results in Fig. 4, because flow cytometry analysis is a technology that allows rapid analysis of millions of cells, generating more statistically reliable data, and is more sensitive than traditional cellular imaging.[29,30] As shown in Fig. 5a, the cells were divided into four groups, the Y axis was the cell counts and the X axis was the fluorescence intensity in log scale. First we set a blank group as control (group 1). The cells treated with Cyto-JN could give faint fluorescence (group 2, treated as described in Fig. 4a). However, the introduction of 100 μM AS to the third cellular system resulted in the first burst of fluorescence response (group 3, treated as described in Fig. 4d). When the fourth cellular system (group 4) was treated with two doses of 100 μM AS, the cells yielded a more significant fluorescence increase than the third group. As shown in Fig. 5b, the statistics of fluorescence intensity exhibited significant differences with each other. These results are consistent with the fluorescence imaging in Fig. 4. The results highlight the ability of our probe to detect intracellular HNO qualitatively and quantitatively.

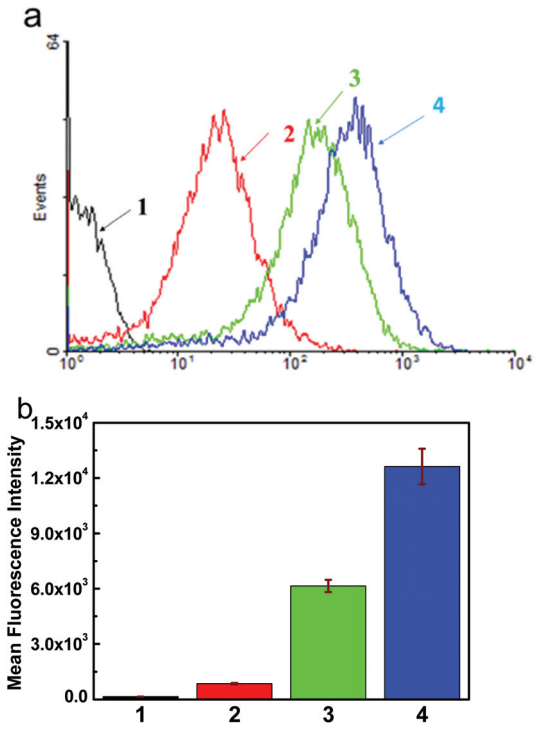

Fig. 5 (a) Representative data of flow-cytometry analysis: (1) blank; (2) the cells were incubated with 5 μM Cyto-JN for 30 min, then washed with DMEM three times to remove the overdose probe; (3) the cells were treated as described in (2), then incubated with 100 μM AS for 30 min; (4) the cells were treated as described in (2) and then exposed to two doses of 100 μM AS for an additional 30 min. (b) Statistical analyses were performed with n = 5, error bars were ± SD.

Bioimaging of HNO *in vivo*

Cyto-JN exhibits high sensitivity, good selectivity, and NIR emission toward HNO detection in cells. In particular, the excitation and emission spectrum in the NIR region can avoid the interference from biological samples, deeply penetrate into tissues, and minimize photo damage to biological samples.[13,18] We next investigated the applicability of Cyto-JN for imaging HNO in living mice using Bruker *In vivo* Imaging System. BALB/c mice were divided into two groups (Fig. 6a). One group (group a) was injected with Cyto-JN (50 μM, 50 μL in 1 : 9 DMSO/saline v/v) into the intraperitoneal (i.p.) cavity; the other group (group b) was first injected i.p. with Cyto-JN (50 μM, 50 μL in 1 : 9 DMSO/saline v/v) and then injected with AS (500 μM, 50 μL in saline) for 30 min. The mice that were incubated with only the probe displayed no fluorescence response (Fig. 6a). However, the mice that were treated with the probe and AS exhibited evident fluorescence increase. The quantification of mean fluorescence intensities for each group is shown in Fig. 6b. The mean fluorescence intensity of group b was ~325 times higher than that of the control group (group a). The results directly indicate that Cyto-JN is capable of imaging HNO *in vivo*.

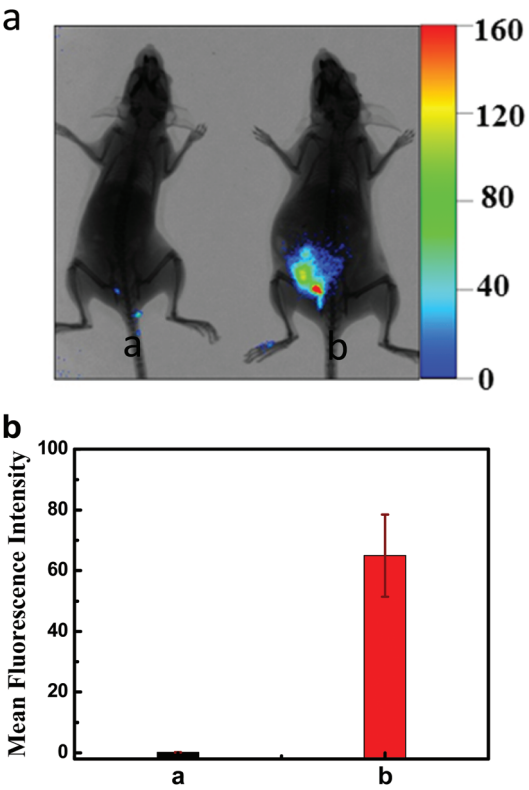

Fig. 6 (a) Fluorescence/X-ray images of BALB/c mice showing HNO level changes using Cyto-JN. Mice in group a were treated with 50 μM Cyto-JN (50 μL in 1 : 9 DMSO/saline v/v) for 30 min in peritoneal (i.p.) cavity. Mice in group b were injected i.p. with 50 μM Cyto-JN for 30 min and then injected with AS (500 μM, 50 μL in saline) for more than 30 min. Images were taken from the 700 nm fluorescence window, λ_{ex} = 680 nm. (b) Quantification of total photon flux from each group. The total number of photons from the entire peritoneal cavity of the mice was integrated. n = 5, error bars were ± SD.

Conclusions

In summary, we demonstrate a new NIR fluorescent probe Cyto-JN for the detection of HNO in cells and *in vivo*. The probe shows high selectivity, good sensitivity, low cytotoxicity, and good cellular penetration for the intracellular detection of HNO. The results of fluorescence bioimaging illustrate that Cyto-JN can be used for the detection of changes in intracellular HNO level. Flow cytometry analysis highlights that the probe can potentially detect intracellular HNO qualitatively and quantitatively. Moreover, Cyto-JN can detect HNO in living mice without interference from background fluorescence. These results suggest that our probe has the potential to be a powerful chemical tool for investigating the effects of HNO during physiological and pathological processes in cells and *in vivo*.

Experimental section

Synthesis of Cyto-JN

Aza-BODIPY (52.9 mg, 0.1 mmol), 2-(diphenylphosphino) benzoic acid (61.2 mg, 0.2 mmol), 4-(dimethylamino) pyridine (24.4 mg, 0.2 mmol), and 1-ethyl-3-(3-dimethylaminopropyl) carbodiimide hydrochloride (19.2 mg, 0.1 mmol) were dissolved in anhydrous methylene chloride and stirred under Ar at 25 °C for 24 h. Then, the mixture was washed by NaBr saturated solution to neutral pH. The organic layer was purified by gel silica column chromatography eluted with CH_2Cl_2. The product was yielded as dark green solid (20 mg, 35%). ^{1}H NMR (500 MHz, DMSO-D_6) δ (ppm): 8.27 (m, 1H), 8.23 (m, 1H), 7.63–7.69 (m, 25H), 7.24–7.22 (m, 19H), 6.97 (s, 1H), 6.43 (s, 1H). ^{13}C NMR (125 MHz, DMSO-D_6) δ (ppm): 169.18, 155.85, 153.51, 151.70, 150.89, 140.15, 140.12, 140.90, 140.68, 137.60, 137.50, 134.33, 134.11, 133.94, 133.57, 131.71, 129.51, 129.44, 129.30, 129.24, 121.43, 120.41, 115.85, 106.78. ^{31}P NMR (200 MHz, $CDCl_3$-D) δ (ppm): −5.54. LC-MS (ESI^+): $C_{70}H_{48}BF_2N_3O_4P_2$ calcd 1105.3181 found $[M + H]^+$ 1106.3260.

Absorption and fluorescence analysis

Absorption spectra were obtained with 1.0 cm glass cells. The Cyto-JN (DMSO, 50 μL, 1 mM) was added to a 10 mL color comparison tube and diluted to 5 μM with HEPES buffer solution (10 mM, 0.5% TW 80, pH 7.4). Fluorescence spectra were obtained with a Xenon lamp and 1.0 cm quartz cells. The probe (DMSO, 50 μL, 1 mM) was added to a 5 mL color comparison tube. After dilution to 5 μM with HEPES buffer (10 mM, 0.5% TW 80, pH 7.4), Angeli's salt (AS, an HNO donor) and other biologically relevant analytes were added. The mixtures in the experiments were incubated for 20 min before measurement.

Cell culture

The mouse macrophage cell line (RAW 264.7) was obtained from the Committee on Type Culture Collection of the Chinese Academy of Sciences (Shanghai, China). The cells were maintained in DMEM supplemented with 10% FBS and incubated in a humidified atmosphere with 5% CO_2 and 95% air at 37 °C. When the cells had reached confluence, they were detached in 0.25% trypsin solution, and then suspended and subcultured in glass bottom cell culture Petri-dishes and allowed to adhere for 24 hours before imaging.

Cytotoxicity assay

The cytotoxicity of Cyto-JN was investigated by the MTT method. RAW 264.7 cells were placed in 96-well cell plates at a final density of 8×10^3 cells per well overnight and treated with different concentrations of Cyto-JN for 24 h. MTT (20 μL 5 mg mL^{-1}) was added to each well and left in the incubator for 4 h, and then the MTT solution was removed and the formazan crystals were dissolved in 150 μL DMSO. The absorbance (OD) of each well was read on a Microplate Reader (Tecan, Austria) at 570 nm wavelength.

Laser scanning confocal microscopy

RAW 264.7 cells were plated in cell culture petri dishes (Φ = 20 mm) with glass bottom at 1.0×10^5 cells per dish with 1 mL of culture medium for 24 h. After the cells were loaded with 2 μM Hoechst 33342 and 1 μM Calcein-AM for 10 min before staining with 5 μM Cyto-JN for 15 min, the culture medium was removed, and the cells were washed twice with DMEM. Then the cells were cultured with 100 μM AS at 37 °C for 15 min. After three washes with DMEM, the cells were examined on a laser scanning confocal microscope with an objective lens (×40), then another 100 μM AS was added as described as above. The spectrally separated images acquired from the three dyes were estimated using Image-Pro Plus software.

Flow cytometry

The cells were cultured at 2.0×10^5 cells per well in 6-well plates and then treated with 5 μM Cyto-JN for 15 min; the cells were further incubated with different concentration of AS for 15 min at 37 °C. After harvest, cells were washed and suspended in DMEM and then analyzed by flow cytometry. Excitation wavelength was 633 nm and collected wavelengths were in the range of 750 nm–810 nm.

In vivo fluorescence imaging

BALB/c mice were obtained from Binzhou Medical University. The mice were group-housed on a 12 : 12 light–dark cycle at 22 °C with free access to food and water. BALB/c mice, 20–25 g, were selected and divided into two groups. BALB/c mice (groups a and b) were given intraperitoneal (i.p.) injections of Cyto-JN (50 μM, 50 μL in 1 : 9 DMSO/saline v/v), then mice (group b) were intraperitoneally injected with AS (1 mM, 50 μL in saline) for 30 min. Finally, two mice were anesthetized by i.p. injections of 4% chloral hydrate (0.25 ml). The two mice were imaged using FX PRO *in vivo* imaging system, with an excitation filter of 680 nm and an emission filter of 700 nm. The results are the mean standard deviation of five separate measurements.

Acknowledgements

We thank the National Nature Science Foundation of China (NSFC) no. 21405172, no. 21275158, the Innovation Projects of the CAS (Grant KZCX2-EW-206), and the Program of Youth Innovation Promotion Association, CAS (Grant 2015170).

Notes and references

1 J. C. Irvine, R. H. Ritchie, J. L. Favaloro, K. L. Andrews, R. E. Widdop and B. K. Kemp-Harper, *Trends Pharmacol. Sci.*, 2008, **29**, 601.
2 N. Paolocci, M. I. Jackson, B. E. Lopez, K. Miranda, C. G. Tocchetti, D. A. Wink, A. J. Hobbs and J. M. Fukuto, *Pharmacol. Ther.*, 2007, **113**, 442.
3 J. C. Irvine, J. L. Favaloro, R. E. Widdop and B. K. Kemp-Harper, *Hypertension*, 2007, **49**, 885.
4 A. Ellis, C. G. Li and M. J. Rand, *Br. J. Pharmacol.*, 2000, **129**, 315.
5 J. C. Wanstall, T. K. Jeffery, A. Gambino, F. Lovren and C. R. Triggle, *Br. J. Pharmacol.*, 2001, **134**, 463.
6 J. C. Irvine, J. L. Favaloro and B. K. Kemp-Harper, *Hypertension*, 2003, **41**, 1301.
7 J. L. Favaloro and B. K. Kemp-Harper, *Cardiovasc. Res.*, 2007, **73**, 587.
8 N. Paolocci, W. F. Saavedra, K. M. Miranda, C. Martignani, T. Isoda, J. M. Hare, M. G. Espey, J. M. Fukuto, M. Feelisch and D. A. Wink, *Proc. Natl. Acad. Sci. U. S. A.*, 2001, **98**, 10463.
9 N. Paolocci, T. Katori, H. C. Champion, M. E. St John, K. M. Miranda, J. M. Fukuto, D. A. Wink and D. A. Kass, *Proc. Natl. Acad. Sci. U. S. A.*, 2003, **100**, 5537.
10 K. M. Miranda, T. Katori, C. L. Torres de Holding, L. Thomas, L. A. Ridnour, W. J. McLendon, S. M. Cologna, A. S. Dutton, H. C. Champion and D. Mancardi, *J. Med. Chem.*, 2005, **48**, 8220.
11 A. S. Dutton, J. M. Fukuto and K. Houk, *J. Am. Chem. Soc.*, 2004, **126**, 3795.
12 (*a*) T. Malinski and Z. Taha, *Nature*, 1992, **358**, 676; (*b*) L. A. Ridnour, J. E. Sim, M. A. Hayward, D. A. Wink, S. M. Martin, G. R. Buettner and D. R. Spitz, *Anal. Biochem.*, 2000, **281**, 223; (*c*) T. Nagano and T. Yoshimura, *Chem. Rev.*, 2002, **102**, 1235.
13 (*a*) E. M. Hetrick and M. H. Schoenfisch, *Annu. Rev. Anal. Chem.*, 2009, **2**, 409; (*b*) X. Q. Chen, Y. Zhou, X. J. Peng and J. Y. Yoon, *J. Chem. Soc. Rev.*, 2010, **39**, 2120; (*c*) X. Li, X. Gao, W. Shi and H. Ma, *Chem. Rev.*, 2014, **114**, 590–596; (*d*) C. E. Paulsen and K. S. Carroll, *Chem. Rev.*, 2013, **113**,

4633; (*e*) Y. Yang, Q. Zhao, W. Feng and F. Li, *Chem. Rev.*, 2013, **113**, 192; (*f*) J. Fan, M. Hu, P. Zhan and X. Peng, *Chem. Soc. Rev.*, 2013, **42**, 29; (*g*) R. Wang, C. Yu, F. Yu and L. Chen, *TrAC, Trends Anal. Chem.*, 2010, **29**, 1004; (*h*) V. Marx, *Nat. Methods*, 2014, **11**, 717; (*i*) M. Gao, F. Yu, H. Chen and L. Chen, *Anal. Chem.*, 2015, **87**, 3631; (*j*) M. Gao, R. Wang, F. Yu, J. You and L. Chen, *Analyst*, 2015, **140**, 3766; (*k*) W. Liu, C. Fan, R. Sun, Y. Xu and J. Ge, *Org. Biomol. Chem.*, 2015, **13**, 4532.

14 (*a*) J. Rosenthal and S. J. Lippard, *J. Am. Chem. Soc.*, 2010, **132**, 5536; (*b*) A. T. Wrobel, T. C. Johnstone, A. Deliz Liang, S. J. Lippard and P. Rivera-Fuentes, *J. Am. Chem. Soc.*, 2014, **136**, 4697.

15 (*a*) M. Royzen, J. J. Wilson and S. J. Lippard, *J. Org. Chem.*, 2013, **118**, 162; (*b*) A. G. Tennyson, L. Do, R. C. Smith and S. J. Lippard, *Polyhedron*, 2007, **26**, 4625; (*c*) L. E. McQuade and S. J. Lippard, *Curr. Opin. Chem. Biol.*, 2010, **14**, 43.

16 (*a*) Y. Zhou, K. Liu, J. Li, Y. Fang, T. Zhao and C. Yao, *Org. Lett.*, 2011, **13**, 1290; (*b*) Y. Zhou, Y. Yao, J. Li, C. Yao and B. Lin, *Sens. Actuators, B*, 2012, **174**, 414.

17 (*a*) U. P. Apfel, D. Buccella, J. J. Wilson and S. J. Lippard, *Inorg. Chem.*, 2013, **52**, 3285; (*b*) M. R. Cline and J. P. Toscanoa, *J. Phys. Org. Chem.*, 2011, **24**, 993.

18 (*a*) L. Yuan, W. Lin, K. Zheng, L. He and W. Huang, *Chem. Soc. Rev.*, 2013, **42**, 622; (*b*) F. Yu, X. Han and L. Chen, *Chem. Commun.*, 2014, **50**, 12234; (*c*) F. Yu, P. Li, G. Li, G. Zhao, T. Chu and K. Han, *J. Am. Chem. Soc.*, 2011, **133**, 11030.

19 J. A. Reisz, E. B. Klorig, M. W. Wright and S. B. King, *Org. Lett.*, 2009, **11**, 2719.

20 J. A. Reisz, C. N. Zink and S. B. King, *J. Am. Chem. Soc.*, 2011, **133**, 11675.

21 (*a*) K. Kawai, N. Ieda, K. Aizawa, T. Suzuki, N. Miyata and H. Nakagawa, *J. Am. Chem. Soc.*, 2013, **135**, 12690; (*b*) Z. Miao, J. A. Reisz, S. M. Mitroka, J. Pan, M. Xian and S. B. King, *Med. Chem. Lett.*, 2015, **25**, 16.

22 X. Jing, F. Yu and L. Chen, *Chem. Commun.*, 2014, **50**, 14253.

23 (*a*) G. Mao, X. Zhang, X. Shi, H. Liu, Y. Wu, L. Zhou, W. Tan and R. Yu, *Chem. Commun.*, 2014, **50**, 5790; (*b*) C. Liu, H. Wu, Z. Wang, C. Shao, B. Zhu and X. Zhang, *Chem. Commun.*, 2014, **50**, 6013.

24 J. Murtagh, D. O. Frimannsson and D. F. O'Shea, *Org. Lett.*, 2009, **11**, 5386.

25 F. Yu, P. Song, P. Li, B. Wang and K. Han, *Analyst*, 2012, **137**, 3740.

26 R. Hu, J. Feng, D. Hu, S. Wang, S. Li, Y. Li and G. Yang, *Angew. Chem., Int. Ed.*, 2010, **49**, 4915.

27 J. Cao, C. Zhao, P. Feng, Y. Zhang and W. Zhu, *RSC Adv.*, 2012, **2**, 418.

28 D. Zhang, W. Chen, Z. Miao, Y. Ye, Y. Zhao, S. B. King and M. Xian, *Chem. Commun.*, 2014, **50**, 4806.

29 L. Frazer, *Environ. Health Perspect.*, 2000, **108**, A412.

30 G. Horstick, T. Kempf, M. Lauterbach, M. Ossendorf, L. Kopacz, A. Heimann, H. A. Lehr, S. Bhakdi, J. Meyer and O. Kempski, *J. Sure. Res.*, 2000, **94**, 28.